ISSN 1062-8738, Bulletin of the Russian Academy of Sciences: Physics, 2021, Vol. 85, No. 10, pp. 1183–1186. © Allerton Press, Inc., 2021.
Russian Text © The Author(s), 2021, published in Izvestiya Rossiiskoi Akademii Nauk, Seriya Fizicheskaya, 2021, Vol. 85, No. 10, pp. 1513–1516.

Modulation Effectiveness of Coronal Mass Ejections with Different Structure of the Magnetic Field

A. V. Belov[a], M. A. Abunina[a, *], E. A. Eroshenko[a, †], A. A. Abunin[a], A. Papaioannou[b], and H. Mavromichalaki[c]

[a] *Pushkov Institute of Terrestrial Magnetism, Ionosphere, and Radio Wave Propagation, Russian Academy of Sciences, Moscow, 108840 Russia*

[b] *Institute of Astronomy, Astrophysics, Space Applications and Remote Sensing, National Observatory of Athens, Penteli, 15236 Greece*

[c] *Faculty of Physics, Nuclear and Particle Physics Department, National and Kapodistrian University of Athens, Athens, 15784 Greece*

**e-mail: abunina@izmiran.ru*

Received May 24, 2021; revised June 1, 2021; accepted June 28, 2021

Abstract—A statistical study of interplanetary disturbances with different positions of the interplanetary magnetic field maximum that generate Forbush decreases is performed. It is shown that the most effective interplanetary disturbances are those with the position of the field maximum 6–15 h after the start of the event.

DOI: 10.3103/S1062873821100075

INTRODUCTION

The effectiveness of different interplanetary disturbances is widely studied because it is of fundamental interest and practical importance [1–4]. The relationship between the structure of interplanetary disturbances and geomagnetic activity is most often studied, but there are also many works dedicated to the effect the structure of coronal mass ejections (CMEs) has on the modulation of cosmic rays (CRs) or (more precisely) the properties of Forbush decreases (FDs) [2, 4–6].

The complete structure of a CME-induced interplanetary disturbance includes the ejection itself, the interplanetary shock wave, and the turbulent zone between them. This structure is reflected in the two-stage character of an FD [7–9]: the first decrease is associated with the arrival of a shock wave; the second, with entering into the ejection itself. It is difficult to avoid subjectivity in selecting and classifying real events. To reduce the influence of subjective factors, we must base the separation of events on objective quantitative parameters.

In this work, we consider the relationship between the structure of large-scale interplanetary disturbances and Forbush decreases in galactic cosmic rays (GCRs). Since GCRs are charged particles, the most important property of the interplanetary medium for them is the magnetic field. The main factor in the structure of the interplanetary disturbance is the distribution of the magnetic field. It is therefore logical to consider the position of the maximum intensity of the interplanetary magnetic field (IMF) in the disturbance as a classifying parameter.

The aim of this work was to identify features and characteristic signs of CME-induced interplanetary disturbances with different structures, based on the position of the IMF maximum, and understand how the structure of the observed disturbances is related to their effectiveness (the ability to generate FDs in CRs and increases in geomagnetic activity).

DATA AND METHODS

We used the database of Forbush effects and interplanetary disturbances created at IZMIRAN [12], which contains data on the main CR parameters (density and anisotropy) obtained through a global survey method for particles with rigidity of 10 GV [10]. It also contains the main parameters of the solar wind (SW) from [13], data on associated solar flares [14] and CMEs [16], SSC time [15], and other parameters.

Our database contains approximately 7500 events, from which we chose FDs (1) with SSCs; (2) with complete data on the IMF (mainly for this reason, we limited to the time period 1996–2017); (3) with separate CMEs as solar sources associated with solar flares; and (4) "pure" events, i.e., those sufficiently far away from neighboring ones. As a result of this selection, only 65 events remained. To increase the probability of disturbances with complete structure, we

† Deceased.

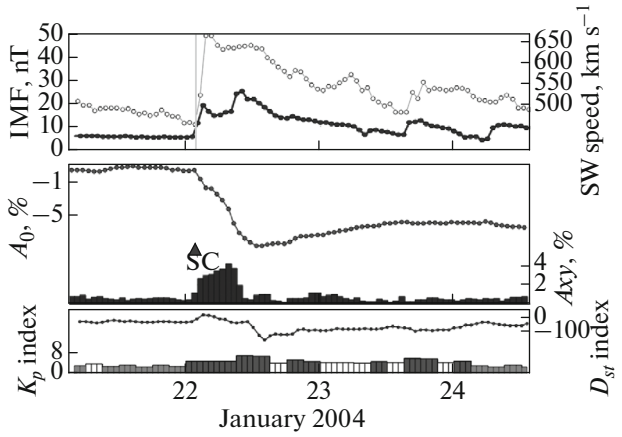

Fig. 1. Behavior of the main parameters of the solar wind, cosmic rays, and geomagnetic activity during the Forbush decrease on January 22, 2004. Top panel: SW speed (right-hand scale, upper curve) and IMF (left-hand scale, lower curve). Center panel: variation of CR density (A_0) (left-hand scale, upper curve) and the equatorial component of CR vector anisotropy (A_{xy}) (right-hand scale, black columns). Bottom panel: measurements of the geomagnetic data (indices D_{st} (right-hand scale, upper curve) and K_p (left-hand scale, columns)). The vertical grey line is the time of SSC detection.

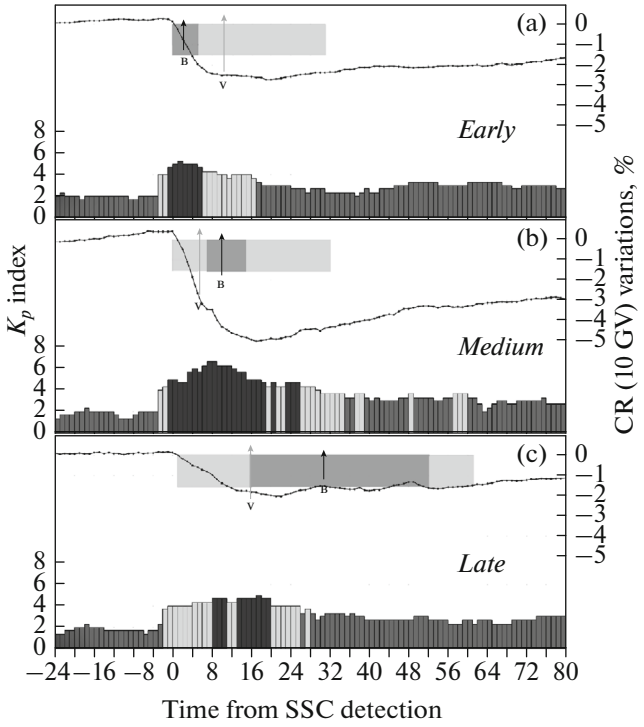

Fig. 2. Superposed epoch (zero hour is the one with the SSC) average behavior of CR variations with rigidity of 10 GV (right-hand scale, black curve) and K_p index of geomagnetic activity (left-hand scale, columns: medium grey for $K_p < 4$, light grey for $K_p = 4$, dark grey for $K_p \geq 5$) for different groups of events: (a) *Early*, (b) *Medium*, (c) *Late*. The arrows show the average position of the maximum IMF intensity and solar wind speed for each group. The regions of the distribution of these maxima are shaded.

chose only FDs associated with central solar sources (−30° to 30°) and obtained 42 fairly confidently identified FDs.

RESULTS AND DISCUSSION

The resulting 42 events with central solar sources were divided into three subgroups according to the time of the IMF maximum (t_B): the *Early* ($t_B < 6$) group included 21 FDs, the *Medium* group ($6 \leq t_B \leq 15$) included 10 events, and the *Late* group ($t_B > 15$) included 11 FDs.

Figure 1 shows an example of the event from the *Medium* group. The top panel of Fig. 1 shows the behavior of the SW speed and IMF, the central panel shows the variation of the CR density (A_0) and the equatorial component of the CR vector anisotropy (A_{xy}), and the bottom panel shows measurements of geomagnetic data (D_{st} and K_p indices). The vertical grey line is the time of SSC detection.

The Forbush decrease on January 22, 2004, began with SSC detection at 01:37 UT. It was a large event with an amplitude of 9%. The CME that caused this FD was very fast (965 km s^{-1}) and associated with the C5.5 flare (S13W09) at 22:02 UT on January 19. The IMF maximum (B_{max} = 25.4 nT) and the FD minimum are close to each other and quite far from the maximum SW speed (V_{max} = 666 km s^{-1}). A large geomagnetic storm was recorded during this event ($K_{p\ max} = 7$, $D_{st\ min} = -149$ nT). The equatorial component of the vector anisotropy in this event was as high as $A_{xy\ max} = 4.32\%$.

Behavior of the Parameters in Different Groups, Averaged Using Superposed Epochs

Let us consider the behavior of the GCR variations and geomagnetic activity, averaged using superposed epochs for different types of CMEs from central solar sources for the *Early* (Fig. 2a), *Medium* (Fig. 2b), and *Late* (Fig. 2c) groups.

In the *Early* group, the maximum SW speed most often lags behind the IMF maximum, while in the other groups it remains ahead. The distribution of the maximum speed is wide in all groups, but it is widest in the *Late* group.

The largest average FD is in the *Medium* group, reaching approximately 5.4%. This value is quite high [11] even for a separate FD, and averaging with superposed epochs underestimates the value of Forbush decreases. The average FD value is lower in the *Early* group (3.1%), and even smaller in the *Late* group (2.1%).

Table 1. Values of the main parameters, averaged using superposed epochs

Group	A_F, %	$K_{p\ \max}$	$B_{\max}$, nT	$t_{B\ \max}$, h	$V_{\max}$, km s^{-1}	$t_{V\ \max}$, h
Early	3.01	5+	18.9 ± 8.0	2.29	564.6 ± 98.8	10.5
Medium	5.4	7	26.4 ± 15.9	10	634.5 ± 183.7	5.5
Late	2.1	5	17.7 ± 5.3	30.9	497.4 ± 85.6	15.7

Table 2. Averaged maximum values of different parameters of the solar wind, geomagnetic activity, and cosmic rays.

	Early ($t_B < 6$)			*Medium* ($6 \le t_B \le 15$)			*Late* ($t_B > 15$)		
Average parameters of the solar wind and geomagnetic indices									
	Mean	Max	Min	Mean	Max	Min	Mean	Max	Min
$B_{\max}$, nT	19.15 ± 1.68	34.6	7.5	26.38 ± 5.04	55.8	12.9	17.74 ± 1.60	24.6	9.1
$V_{\max}$, km s^{-1}	567.4 ± 20.7	774	449	634.5 ± 58.1	959	391	497.4 ± 25.8	677	409
$K_{p\ \max}$	5.24 ± 0.32	7.3	2.3	6.30 ± 0.63	8.7	3.3	5.64 ± 0.31	7.3	4.3
$A_{p\ \max}$, nT	66.14 ± 11.34	154	9	128.70 ± 31.45	300	18	74.00 ± 12.07	154	32
$D_{st\ \min}$, nT	−60.3 ± 7.3	−132	−22	−133.9 ± 40.6	−422	−4	−79.6 ± 13.0	−159	−26
Average parameters of cosmic rays									
	Mean	Max	Min	Mean	Max	Min	Mean	Max	Min
A_F, %	3.52 ± 0.50	9.4	0.9	5.66 ± 0.81	12.3	2.7	2.87 ± 0.59	8.9	0.9
$D_{\min}$, %	−0.76 ± 0.11	−1.97	−0.21	−1.15 ± 0.28	−3.40	−0.46	−0.49 ± 0.06	−0.81	−0.16
$A_{xy\ \max}$, %	2.00 ± 0.15	3.81	1.15	2.69 ± 0.32	4.35	1.60	1.83 ± 0.12	2.45	1.31
$A_{z\ range}$, %	2.16 ± 0.18	4.51	1.00	2.32 ± 0.23	3.68	0.99	2.55 ± 0.47	5.29	1.34

The magnetic storm in the *Medium* group is not only the largest (strongest), it is also the longest: the storm level (K_p around 5 and above) persists for approximately a day, and the disturbed level (K_p around 4) is observed more than two days after the start of the event. In other groups, the averaged magnetic storm (small) ends much faster, especially in the *Early* group (after only 6 hours). The geomagnetic activity in the *Late* group is more prolonged. All the above parameters are summarized in Table 1.

Averaged Extreme Parameters

Table 2 shows the average values of different parameters of the solar wind, cosmic rays, and geomagnetic activity for the selected groups. The parameters of the solar wind and geomagnetic activity are the maximum IMF intensity, $B_{\max}$; the maximum SW speed in the event, $V_{\max}$; and the extreme values of the geomagnetic indices ($K_{p\ \max}$, $A_{p\ \max}$, $D_{st\ \min}$). The CR parameters are the FD magnitude A_F; the maximum hourly decrease in CR density $D_{\min}$; the maximum value of the equatorial component of the CR vector anisotropy $A_{xy\ \max}$; and the variation in the A_z component of CR anisotropy, $A_{z\ range}$.

Table 2 shows that the *Medium* group stands out markedly in almost all parameters, relative to the two other groups. It has the highest average values for all parameters of the solar wind ($B_{\max}$, $V_{\max}$) and geomagnetic activity ($K_{p\ \max}$, $D_{st\ \min}$). It also contains the largest FDs with the highest values of the equatorial component of CR anisotropy. The only parameter in which the *Medium* group is inferior to the *Late* group is the variation in the A_z component of anisotropy, but this excess is negligible (within the statistical error).

CONCLUSIONS

The time of the IMF maximum is an important parameter that can be used to classify Forbush decreases and associated solar wind disturbances. Events with central solar sources were divided into three groups, according to the time of the IMF maximum (t_B): *Early* ($t_B < 6$), *Medium* ($6 \le t_B \le 15$), and *Late* ($t_B > 15$). Considerable differences between the groups in terms of the characteristics of the solar wind, geomagnetic activity, and cosmic rays were revealed.

Forbush decreases with the position of the IMF maximum 6–15 h after the start of the event were accompanied by the highest values of the main parameters of the solar wind, geomagnetic activity, and cosmic rays.

FUNDING

The work of A.V. Belov, M.A. Abunina, and A.A. Abunin was supported by the Russian Science Foundation, project no. 20-72-10023.

REFERENCES

1. Gopalswamy, N., Akiyama, S., Yashiro, S., et al., *J. Atmos. Sol.-Terr. Phys.*, 2008, vol. 70, p. 245.
2. Dumbović, M., Vršnak, B., Čalogović, J., and Župan, R., *Astron. Astrophys.*, 2012, vol. 538, A28.
3. Chertok, I.M., Grechnev, V.V., Belov, A.V., and Abunin, A.A., *Sol. Phys.*, 2013, vol. 283, p. 557.
4. Belov, A., Abunin, A., Abunina, M., et al., *Sol. Phys.*, 2014, vol. 289, p. 3949.
5. Dumbović, M., Vršnak, B., Čalogović, J., and Karlica, M., *Astron. Astrophys.*, 2011, vol. 531, A91.
6. Belov, A., Abunin, A., Abunina, M., et al., *Sol. Phys.*, 2015, vol. 290, p. 1429.
7. Barnden, L., *Proc. 13th Int. Cosmic Ray Conf.*, Denver, 1973, vol. 2, p. 1277.
8. Belov, A.V., Dorman, L.I., Eroshenko, E.A., et al., *Geomagn. Aeron.*, 1976, vol. 16, no. 5, p. 761.
9. Wibberenz, G., Le Roux, J.A., Potgieter, M.S., and Bieber, J.W., *Space Sci. Rev.*, 1998, vol. 83, p. 309.
10. Belov, A., Eroshenko, E., Yanke, V., et al., *Sol. Phys.*, 2018, vol. 293, p. 68.
11. Belov, A.V., Eroshenko, E.A., Oleneva, V.A., et al., *Adv. Space Res.*, 2001, vol. 27, p. 625.
12. http://spaceweather.izmiran.ru/eng/dbs.html.
13. http://omniweb.gsfc.nasa.gov.
14. ftp://ftp.swpc.noaa.gov/pub/indices/events.
15. http://isgi.unistra.fr/data_download.php.
16. https://cdaw.gsfc.nasa.gov/CME_lis.

Translated by M. Chubarova